Engineering and Technology Journal e-ISSN: 2456-3358
Volume 07 Issue 10 October-2022, Page No.-1544-1562
DOI: 10.47191/etj/v7i10.02, I.F. – 6.484

Analysis of Seepage Through The Dam Considering Various Soil Characteristics Using an Experimental and The Finite Element Modeling Technique

T. E. Okeke [1], F. C. Onyeka[2], Sule Joseph[3]
[1]Department of Civil Engineering, University of Nigeria, Nsukka, Enugu State, 410101, Nigeria.
[2,3]Department of Civil Engineering, Edo State University Uzairue, Edo State, 312102, Nigeria.

ABSTRACT: In this study, the rate of seepage flow through the dam was investigated using both experimental and numerical modeling techniques. Two different types of soil samples were collected at a depth of 1m from the Auchi site in Edo State, Nigeria. The soil samples were subjected to preliminary tests such as the sieve analysis, the limit state (liquid limit, plastic limit and plasticity index), and the specific gravity test. Notable differences in the Geotechnical properties of two samples of soils were observed. The sieve analysis indicated that the particles passing through a 200-sieve number of size 0.075mm were 14.32% and 13.48% respectively. The liquid limit of sample 1 and sample 2 was determined to be 35% and 30%, the plastic limit 20.5% and 24.3%, the plasticity index 14.5% and 5.7% and the specific gravity of the two samples 2.63 and 2.65 respectively. Shear test was conducted to obtain the bearing capacity of soil using Terzaghi principle thereafter, the finite element analysis was used by applying SEEP/W of the Geo Studio program to determine the rate of flow of seepage through the dam. The result of the analysis showed that earthen dam without considering the core gave 12% difference in the seepage through the earthen material, the core of hydraulic conductivity 10 times less than that of the homogenous material gave 19.06% percentage difference seepage rate of flow with consideration of core with k 10 times less than homogenous material and the core of hydraulic conductivity 100 times less results gave 17.86% percentage difference for core of k 100 times less than homogenous material. Recommendations were made based on these results to reduce the rate of flow of seepage through the dam.

KEYWORDS: Rate of seepage flow through the dam, Analysis of bearing capacity of soil using Terzaghi principle, Experimental and finite element analysis of seepage, SEEP/W of the Geo Studio application in finite element method.

1. INTRODUCTION

A dam is a structure built over a river or stream to control, store, or redirect water. It can be made of concrete, earth, or steel (Wong, 2013). According to whether the height (H) of the crest level above the waterbed level is lower or higher than fifteen meters, i.e., for small dams, H15 m, and for large dams, H>15 m, they are commonly categorized as small or large dams (Awomeso *et al.*, 2009). According to the type of material used in their construction, dams can be categorized. In Nigeria, the most prevalent types of dams are embankment dams, which are made of earth fill and/or rock fill, and concrete dams (Okusun and Amadasu, 2016). Building a dam across the river results in the creation of a sizable man-made lake. Seventy-nine percent of dam have domestic and industrial water supply components, while 33% have irrigation as a major use to which the stored water is put; 29% are for fisheries, 16% for recreation and 4% are also for hydroelectric power generation (HEP) (Oke and Abubakar, 2013).

A flood occurs when water overflows and engulfs normally dry territory. The tide's inflow is another example of streaming water. Levees and other flood barriers, as well as wider environmental issues like climate change and sea-level rise, are all known to enhance the intensity and frequency of floods. Land-use changes like deforestation and the destruction of wetlands also increase flooding (Watanabe *et al*., 2013). Significant consequences of flooding include the loss of life, damaged properties, oil production, agricultural and damage to buildings and infrastructure like bridges, sewage systems, roads, and canals (Magami *et al*., 2014). According to estimates, Nigeria's losses from flood occurrences in 2012 alone totaled more than $16.9 billion in terms of property destruction, lost oil output, agricultural losses, and other losses (Amangabra and Obenade, 2015). Numerous lives and homes have continued to be at risk due to an increase in flood events, a lack of coping mechanisms, and a high level of vulnerability among the populace (Komolafe *et al.*, 2015).

Seepage flow is a fluid (water) passage through porous soil layers such as sand in hydrology. As a result of gravity, the fluid fills the pores in the unsaturated bottom layer and travels into the deeper layers, the soil must be porous so that seepage water does not accumulate (Uromeihy *et al.,* 2007). The permeability coefficient of in m/s describes the permeability of the soil and is affected by grain size and usable pore space. Seepage water can be temporarily stored in less permeable soils. If seepage water comes into contact with an impervious soil layer of impermeable rock, seepage ceases and seepage water accumulates permanently. Groundwater is the term for such underground water accumulations. We talk about groundwater when the water resource is available all year, drinking and mineral water are made from groundwater, which is a natural resource. It also serves as a vital buffer in the overall water cycle

The flow mechanisms occur in water-saturated soil layers, groundwater, and stored water, as well as in seepage water above the groundwater Water flow in the soil is caused by potential differences. Water always goes from locations of higher potential, i.e. more potential energy, to points of lower potential in this situation. The water will continue to travel until the potentials reach a point of equilibrium. A potential equilibrium is constantly disrupted by precipitation, groundwater extraction, and evapotranspiration (evaporation from the free surface and release of water vapor from plants). Soil water rarely reaches a state of balance in a static state. The permeability of the soil through which water is flowing is also important (Earle, 2015).

Seepage analysis is a useful tool for predicting seepage and determining how to prevent or lessen the amount of seepage flow. The seepage analysis in the earthen dam is carried out to analyze the phreatic line, the pore pressure within the dam or in its foundation, the exit gradient at the dam's downstream face, and the amount of seepage flow that may pass through the dam's cross-sections in most of these (Salem *et al.*, 2019). The seepage analysis is carried out by various analytical methods and numerical approaches such as finite element method (FEM) to determine the amount of seepage through the earth dam. The FEM provides the solution of seepage problems faster and complex seepage problems can be solved utilizing FEM in seepage analysis. The seepage problem of an earth dam has been solved by several writers using FEM to guarantee the application of FEM based solutions to the seepage problem of an earth dam, it is necessary to check the consistency of the analytical and FEM-based answers. All boundary conditions are known in practically all issues involving seepage behind sheet pile walls or through the foundation of a dam; but, in the case of seepage through an earth dam, the top boundary or uppermost flow line is unknown and must be discovered first, adding to the complexity. The line of seepage will be defined as the upper border, which is a free water surface (Olonade and Agbede, 2013).

Losses from dam flow must be minimized, and seepage flows that could affect pipework must be managed. Dams can be equipped with a variety of seepage control methods to prevent failure (Torabi *et al.*, 2020). To prevent excess seepage from causing water under pressure to well up through a bed of sand, the water appears to be boiling up from the bed of sand, seepage analysis is an essential and necessary part of the structural analysis in the design of any dam (Adamo *et al.*, 2020). Continuous piping can cause enough material to exit through the boil to build a huge gap inside the dam, weakening the structure and finally causing it to fail. Although not all sand boils result in dam failure, they are the most common cause of dam failure. More so, an excessive seepage pressure may be causing a slope to become saturated and create slips. Seepage that is not regulated can weaken the soil and cause structural failure. A structural collapse could shorten the seepage path, resulting in piping failure. Surface erosion has the potential to cause structural failure (Manning, 2016).

Solutions for groundwater seepage problems have been developed from the pioneering work of Henry Darcy from Darcy's law, a formula for predicting the flow of a liquid through a porous media with states that the discharge rate q is proportional to the gradient in the hydraulic head and the hydraulic conductivity.

$$q = \frac{Q}{A} = -K * \frac{dh}{dl} \qquad (1.1)$$

Groundwater is the water in the saturated zone and consists of about 30% of fresh water on earth below the surface, groundwater flow is the flow of water through a porous medium or tortuous flow, here the frictionless flow is totally meaningless, and gradients in potential energy, drive groundwater flow as it flows from high elevation to low elevation and from high pressure to low pressure (Earle, 2015).

Less than 1% of the Earth's water are available for human use, the average family uses 400 gallons of water daily and expected population growth means an increase in water use. The study of hydrology and how water behaves as it moves through the water cycle is vital to reducing strain on our water supply and infrastructure (Chu-Agor *et al.*, 2008). The groundwater seepage problem can be described by Darcy's Law and continuity equations. The seepage equation is obtained by combining these two equations. Since the seepage equations are based on these two equations, the assumptions and limitations that apply to these equations also apply to the seepage equation. Darcy's law basically demonstrates a linear dependency between the hydraulic gradient and the discharge velocity. Several investigators such as Dupuit; Schaffernak; Casagrande over the years have suggested various methods to evaluate the amount of seepage and the phreatic line's location.

Earth dams have always been associated with seepage as they seep water into it. The water has looked for the paths of least resistance through the earth dam and its foundation (Panthulu *et al.*, 2001). Several investigators have suggested various methods to determine the quantity of seepage through an earth dam without a filter.

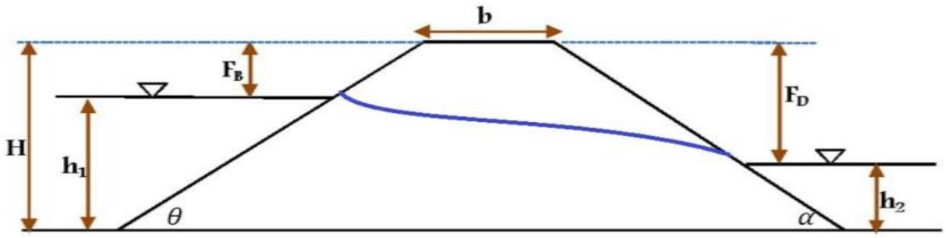

Fig 1.1. General section of homogenous earth dam without filter

Dupuit by assuming that aquifer is homogeneous, isotropic and of infinite aerial extent, the velocity of flow is proportional to tangent of hydraulic gradient and not sine, the flow is horizontal and uniform throughout the vertical section, entire thickness of aquifer is contributing water to the well, coefficient of transmissibility remains constant at all places and all the time, flow is laminar, ground water conditions remain constant all the time, hydraulic gradient is constant and utilizing Darcy's law to determine the discharge rate passing for each vertical profile of the dam (Das, 2008).

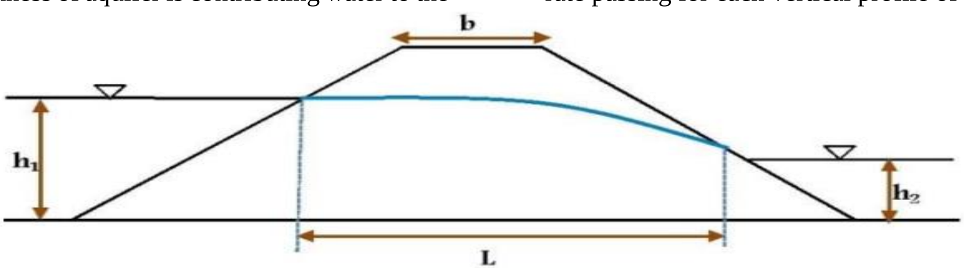

Fig 1.2 Dupuits solution for flow through earth dam

Abdul (2016) in a research work had shown that Schaffernak had developed an approximate method to calculate the seepage through a homogeneous earth dam with zero downstream head by suggesting that the phreatic surface has intersected the downstream slope at a distance from the impervious base as seen in the equation 2.85.

Salmasi and Abraham (2021) conducted a validity study showing Casagrande calculation the amount of seepage through the body of a homogeneous earth dam that was constructed on an impervious foundation, for the case of zero downstream head, and helps make an adjustment for the entrance condition at the upstream face by implying that the parabolic free surface begins at a point upstream, where (Δ) is equivalent to the base width of the upstream triangular part.

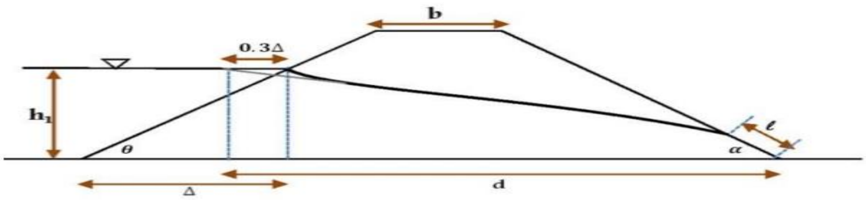

Fig 1.3. Casagrande's solution for flow through an earth dam

Emeka and Chukwuemeka (2019) in a research work modified Schaffernaks' approach for seepage through earth dams, emphasizing the significance of understanding the distribution of seepage uplift pressures and associated seepage forces, as well as estimating the volume of seepage losses through the body and foundation of earth dams.

The Finite Element Method (FEM) is a technique for solving equations that underlie problems in nature quantitatively. It is a numerical method that provides approximations to the solutions of differential equations used to address physics and engineering issues. The finite element approach calls for a problem defined in geometrical space or domain to be divided into a limited number of smaller regions, just like in straightforward finite difference methods (Darrel *et al.*, 2006). FEM's greatest strength is its ability to apply to any irregular geometry with a variety of boundary conditions.

The software PLAXIS 3D based on FEM is used by Bayat *et al.* (2019) to determine the transient seepage analysis on the subject earth dam for 1 year in order to understand the function of such structures. The results from seepage at the same places with 15-day intervals across a one-year experimental sample are compared with the outputs in the downstream drain.

Kacimov *et al.,* (2021) examined seepage through a zonal earth-filled dam with a vertical clay core, two permeable shoulders, and a toe drain. The downstream shoulder and seepage through the core are linked. The phreatic surface and flow rate are discovered. With the hodograph approach, a complicated potential plane rectangle is conformally mapped into a circular triangle. Using streamline refraction at the intersections of the core and both shoulders, MODFLOW 2005 numerically simulated seepage but the research didn't consider dams made of different earthen materials and the effects it may have on the seepage flow.

Li *et al*. (2003) developed an element-free method (EFM) for seepage analysis using a free surface based on the moving least square approach, which only requires node information. It avoids the finite element method's time-consuming mesh change. The quadratic mesh is stable during the iterations of computing the free surface since it is relative to the nodes. In the iterations, the nodes can be simply added, moved, or removed. Considering the original free boundary problems as a problem of shape optimization performed a boundary element discretization (Leontiev and Huacasi, 2001). A mathematical programming technique for numerical simulation of unconfined flow through porous media was presented. Taking the state variable and free boundary variable as independent variables they treated.

The method was applied to analyze the steady seepage in the foundation pit, a lock foundation, and an embankment dam with a free surface (Jie *et al.*, 2004). Jairry (2010) conducted a study on 2D- flow analysis through the zoning earth day using CivilFEM/ANSYS(11) software to predict two-dimensional steady-state water seepage through an earth dam of two soil zones resting on the impervious base. It has been applied to a variety of issues (Hoffman, 2001). These include time-independent and dependent, linear and non-linear issues. This approach can be used to solve issues involving various boundary conditions and boundary forms (Zhou, 2012). With the finite-difference method, you may easily run into problems handling curved boundaries for the purpose of defining the boundary conditions. Boundary conditions are needed to truncate the computational domain.

Malkawi *et al.* (2000) located the probable sources of the Kafrein dam seepage problem taken into account a technique called excitation-response analysis. From a linearized groundwater flow equation for one-dimensional semi-infinite, isotropic, and homogeneous porous media, analytical equations that show the groundwater level reaction in the underlying aquifer as a result of changes in the reservoir water level were produced. The findings showed that a significant amount of seepage water starts from a location about 1 km from an observation point M1 and streamlines along the active faults. The result was achieved through only the finite difference method of analysis without considering other methods such as the finite element method for numerical analysis.

Prior to construction, Uromeihy *et al.* (2007) looked into the engineering, geological characteristics of the land at the Chapar-Abad Dam to assess seepage issues and choose the best waterproofing strategy. The potential for water seepage was assessed by the examination of the joint systems between rock units, the application of numerical analysis to predict groundwater flow, and the execution of in-situ tests to determine the values of permeability. The researchers conducted the groundwater flow for the dam without looking at the effects of an impervious core.

The finite difference method (FDM), a five-point approximation method, was introduced by Kermani and Barani (2012) as a solution to the seepage issue with earth dams. By numerically solving the Laplace equation, the grid system was created, with the computational border corresponding with the physical boundary. The technique was used to examine the constant seepage in an earth dam. Three alternative grid types were taken into consideration in this investigation, and the conclusions were contrasted with those drawn from an analysis using the Geostudio 2007 program. It demonstrated that by selecting modest enough increments, the outcomes are acceptable.

In a research work on comparative analysis of seepage through the dam Arinze and Aguwamba (2010) used analytical methods (Schaffernack's and L-Casagrande's methods) and numerical methods (FEM). Another comparison analysis by Sazzad *et al.* (2014) on the analytical and numerical solutions of seepage flow through an earth dams using analytical solutions, the seepage through an earth dam was estimated, noting the limitations or disadvantages of the analytical solution, that it requires many assumptions and only simple and straightforward seepage problem can be solved. The important advantage of using the finite element method (FEM) in seepage analysis is that the solution to seepage problems is faster and complex seepage problems can be solved using FEM (Arinze and Aguwamba, 2010). A noticeable reduction of the discharge rate is observed with the addition of clay core in the model. It should be noted that the upstream and downstream angle has no effect on discharge rate when an internal clay core was used (Sazzad *et al.*, 2014). Using the computer program SEEP/W, Abdul (2016) conducted research on the amount of seepage through a homogeneous earth dam without a filter that was lying on an impervious base (which is a sub-program of Geo-Studio). SEEP/W experiments are conducted with three different downstream slopes, three different upstream slopes, three different downstream heads, three different upstream heads, three different heights of earth dams, and three different top widths of earth dams. The amount of seepage has been calculated for each run. To establish an empirical equation to calculate the amount of seepage through a homogeneous earth dam resting on an impermeable base, dimensional analysis was employed with the aid of theoretical findings. Additionally, use an artificial neural network (ANN) to confirm the SEEP/W results and compare with other analytical techniques. Yields reveal that Dupuit's solution has more than 20 percent error and Casagrande's solution has more than 15 percent error when compared to the suggested equation with artificial neural network (ANN) with less than 3 percent error and SEEP/W results with less than 2 percent error.

In this research, geotechnical properties of the soil was carried out and bearing capacity of soil on a homogenous dam entirely composed of one material with steady flow through the earth dam was evaluated experimentally thereafter, a FEM analysis was done using the SEEP/W software of Geo Studio program was performed for three dimensional steady-state water seepage through an earth dam of two soil zones resting on the impervious base to determine the rate seepage flow through an earth dam for the two different types of soil. In this study, sixty numerical models of earth dams have been analyzed without and with clay core and a more suitable method of reducing seepage through the dam is recommended to excessive leakage into the surrounding soil causes sand boils which weakens the soil structure and can lead to soil liquefaction when saturated thereby causes the dam structure to fail.

2. MATERIAL AND METHOD

The research methodology involves preliminary test and numerical analysis. The materials required for the laboratory work of this study are samples of two different types of soil collected at a depth of not less than 1.0m below the ground surface from Auchi town in Edo state and various experiment were being carried out to get Geotechnical properties of the soil. The preliminary tests which include: sieve analysis, consistency/limit state analysis and specific gravity test were performed to obtain the suitable soil parameters and structures to be erected the preliminary test were carried out in accordance with British Standard (BS) code of practice (BS 1377, 1975; BS 1377, Part 2, 1990; BS, 812-103.1, 1985). The soil samples are to be classified according to AASHTO (ASTM, 2006) and USCS methods of soil classification (Onyeka, 2019; Onyeka and Osegbowa, 2020). Thereafter, shear test was conducted in the laboratory to determine the bearing capacity of the soil when subjected loading. Furthermore, a numerical analysis using the SEEP/W of the Geo studio, which is a Finite element method (FEM) program was performed using data acquired from the laboratory work to determine the rate of flow of seepage.

2.1 Sieve Analysis

The grading of aggregates to ascertain the distributions of particle sizes, is called sieve analysis to determine whether the soil consists of predominately gravel, sand, silt or clay sizes and to a limited extent which of these size ranges is likely to control the engineering properties of soil. A total of 250g of soil sample was weighed out from direct soil (undisturbed sample) and placed on a tray and allowed to dry by oven drying in a thermostatically controlled oven maintained at about 110^{0}C. After drying the sample was placed in the topmost sieve and is shaken long enough that all particles smaller than each sieve size can pass through. This was achieved by using the mechanical sieve shaker. A set of sieve was arranged according to their sizes to the smallest size of 0.063mm with the receiving pan was placed in the shaker, the dried soil sample was placed in the top sieve and air-dried and placed in a set of sieves arranged in ascending order. The material retained on each sieve was transferred to a weighed container. The dried sample was poured on top and agitated for a few seconds and sample mass retained on each sieve were collected, weighed and recorded. Grain size analysis expresses qualitatively the proportion by weight of the various sizes of particles present in the soil or aggregate down to the fine sand by dry sieving. Apparatus**:** Stacks of test sieves, a set of sieves, brush (for cleaning sieves), weighing balance (with accuracy to 0.01g), Rubber pestle and mortar (for crushing the test material if lumped or conglomerated), large pan and riffle box, sieve shaker and oven. Thereafter, the percentage retained, passing and coefficient of curvature/uniformity was calculated according to Tezaghi *et al.* (1996). For a well graded soils, it was reported that Cu ≥ 6 and 1< Cc 3.

$$\text{Percentage retained} = \frac{\text{mass Retained}}{\text{Total mass retained}} \times 100 \qquad (2.1)$$

$$\text{Percentage passing} = 100 - \text{Percentage retained.} \qquad (2.2)$$

$$\text{Coefficient of curvature (Cc)} = \frac{(D_{30})^2}{D_{60} \times D_{10}} \qquad (2.3)$$

$$\text{Coefficient of uniformity (Cu)} = \frac{D_{60}}{D_{10}} \qquad (2.4)$$

2.2 Specific Gravity

The specific gravity of soil was conducted, the Specific gravity of soil generally ranges from 2.60 to 2.90 to aid soil classification and identification. A specified quantity for the test, for the two soil sample was weighted out, and the test was carried out, in accordance with specifications. At the end of the experiment, values were recorded and calculations carried out. It entails weighing density bottles, recording the weight as (W1) g, and sieving some cooled oven-dried sample through a 425-m sieve. The density bottles were filled with certain sieved materials and weighed as (W2) g. Following the addition of distilled water, the sample-filled bottles were shaken to guarantee the removal of any air before being left for 24 hours. The bottle and its contents are shaken before being weighed as W3 (g). The density bottles were cleaned, filled with distilled water exclusively, and weighed as W4 after being empty for 24 hours (g). Each bottle's specific gravity was calculated based on the readings, and the average result was used as the specific gravity. Apparatus: density bottles, weighing balance, funnel, and 25μm sieve. The sensitive pycnometer/density bottle method, which is characterized by several complexities and challenges, is used to determine the specific gravity of soil in laboratories (Prakash *et al*., 2012). The specific gravity is computed in accordance to Hosni *et al.* (2015) as:

$$\text{Specific Gravity (Gs)} = \frac{W_2 - W_1}{(W_4 - W_1) - (W_3 - W_2)} \tag{2.5}$$

Where;

W_1 = Weight of density bottle, W_2 = Weight of density bottle + sample of soil, W_3 = Weight of density bottle+ soil sample + water, W_4 = Weight of density bottle + water.

2.3 Limit State Analysis

A sample of the soil is air dried and sieved through the sieve of size 0.425 mm, thoroughly mix the soil with a small amount of distilled water until it appears as a smooth uniform paste, weigh four of the empty moisture cans with their lids, and record the respective weights. Adjust the liquid limit apparatus by checking the height of drop of the cup. Recording the number of blows required for each sample, determining the water content for each trial and plotting the graph to get the liquid limit at 25 blows.

For the Plastic limit the remaining soil sample is weighed and recorded, adding water to the soil until it is at a consistency it can be rolled without sticking to the hand, when the diameter of the thread reaches the correct diameter, break the thread into several pieces. Knead and reform the pieces into ellipsoidal masses and re-roll them continuing until the thread crumbles under pressure required for rolling, gathering the portions of the crumbled thread together and place the soil is not a moisture can record the mass and place in oven for about 16hrs for each trials computing the water content of each trial.

$$\text{PL} = \frac{Weight\ of\ water}{\text{Weight of over} - \text{dry soil}} \times 100 \tag{2.6}$$

$$Plasticity\ Index\ (PI\ \%) = \text{PI} = \text{LL} - \text{PL} \tag{2.7}$$

Where LL and PL are the Liquid and plastic limits respectively

2.4 Numerical Modelling using GeoStudio

The Geo Studio computer programmed is a boundary-valued problems and were used in this study to evaluate the performance of dams and levees with varying levels of complexity in order to simulate seep through the soil in both saturated/ unsaturated condition of the soil, the distribution of pore water pressure saturated and unsaturated zones. The scope of the study is steady state low through saturated/unsaturated material. The only apparatus needed is the SEEP/W modeling of the Geo Studio software.

Procedure: The entire analysis can be broken down to several basic functions of the SEEP/W which includes the definition view, solver manager, result view and interpretation of results and then print analysis in page layout mode. The object information tool in the Geostudio provides information on each geometry item such as the boundary conditions or the mesh properties of a region while the view result information provides details for a node, flow path, gas region. The graph for the seepage analysis can be plotted using the graphical tool for seepage analysis the conductivity against metric suction helps to assess convergence of the analyses and also the pore water pressure graph through the middle of the embankment. The SEEP/W can also be used to find out what would happen to the phreatic surfaces given the pressure of a toe dam by cloning the already selected parameters from the first analysis, but adding a boundary condition to represent the presence of a toe drain, then creating finer discretization of 0.5m along the toe drain as our phreatic surface is expected to fall along this line. **Apparatus/Required Components:** the geometry or region for the embankment (dam), and the material properties which include the volumetric water content and hydraulic conductivity of the homogenous material for the dam, and the boundary conditions. The boundary conditions for the modelling includes the drainage or potential seepage face, the reservoir level chosen a constant water head value according to the level of the reservoir and the zero pressure boundary condition.

2.4.1 Assumptions of Numerical Modelling Technique

For the numerical modelling various assumptions were made such as:

i. The hydraulic gradient is constant along the vertical line (flow is horizontal)
ii. Hydraulic conductivity is for homogenous material is constant

iii. Soil in the flow field is homogenous (made entirely of one material)
iv. The exit point coincides with the tail water
v. The foundation of the dam is not considered only seepage flow through the embankment
vi. Pore water is compressible

2.4.2 Parameters for Design Model

The Figure 2.1 gives a representation of a design model, the parameters above are:

Height of the Dam H which is 9m, total water head h from the base of the dam to the top of the reservoir which is 8m, top width of the dam W which is 4m, the Base of the embankment which is 35m, the toe drain width of 6m, the Upstream slope (US) of 1.7:1, the downstream slope (DS) of 1.5:1.

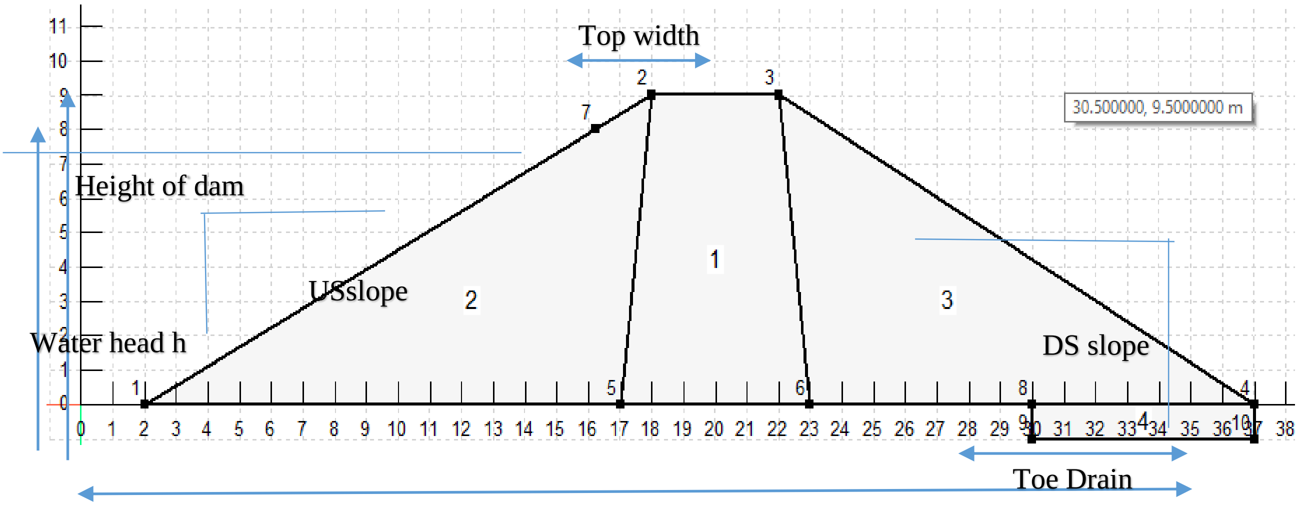

Fig 2.1. A proposed dam design model

Base of embankment

3. RESULTS AND DISCUSSION

3.1 Sieve Analysis Data for Sample 1: Weight of dry sample (g) = 250g

Table 3.1: Sieve analysis for sample 1

Sieve number	Sieve opening (mm)	Mass of soil retained on each sieve (g)	Percentage mass retained on each sieve	Cumulative percent retained	Percentage Passing
4	4.75	6.2	2.48	2.48	97.52
8	2.36	27.0	10.8	13.28	86.72
10	2.00	10.4	4.16	17.44	82.56
16	1.18	39.1	15.64	33.08	66.92
30	0.60	23.6	9.44	42.52	52.48
40	0.425	15.8	6.32	48.84	51.18
50	0.30	52.4	20.96	69.80	30.20
100	0.15	18.8	7.52	77.32	22.88
200	0.075	20.9	8.38	85.70	14.32
pan	0	36.8	14.32	100.00	

Percentage coarse aggregate is the percentage passing through size NO 4 (4.75mm) which is given at 2.48%; percentage of medium is given as 100- (14.32+ 2.48) =83.2% and percentage fine aggregate is the percentage passing through the sieve NO 200 (0.075mm) which is 14.32%.

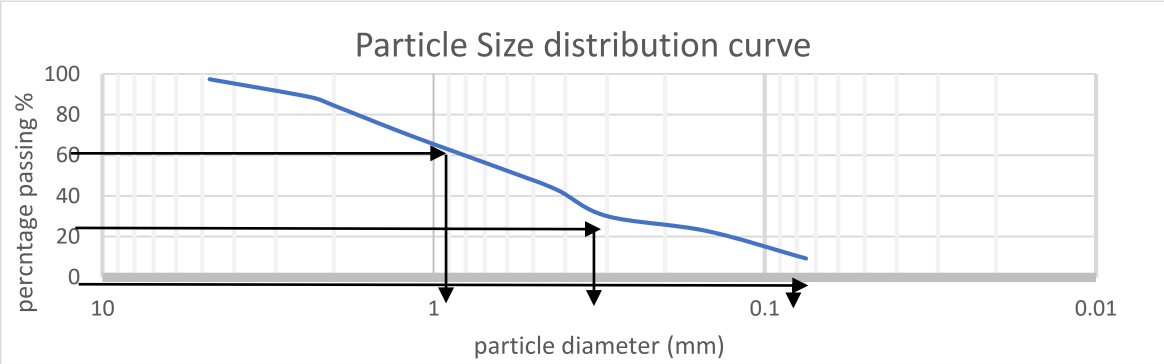

Fig 3.1. Graph for particle size distribution for sample 1

From the above graph it is determined that:
$D_{10} = 0.075$, $D_{30} = 0.29$, $D_{60} = 0.80$, $C_U = 10.67$, $C_C = 1.4$

Where D_{10}, D_{30}, D_{60} are the percentage passing through the sieve, C_u and C_c are the coefficient of curvature and uniformity respectively.

3.2 Sieve Analysis data for sample 2: Weight of dry sample (g) = 250g

Table 3.2. Sieve analysis for sample 2

Sieve number	Sieve opening	Mass of soil retained on each sieve (g)	Percentage mass retained on each sieve	Cumulative percent retained	Percentage Passing
4	4.75	6.60	2.64	2.64	97.36
8	2.36	14.8	5.84	8.48	91.52
10	2.00	46.8	18.72	27.20	72.80
16	1.18	14.1	5.64	32.84	67.18
30	0.60	19.0	7.60	40.44	69.66
40	0.425	20.8	8.32	48.76	61.24
50	0.30	51.6	20.64	69.40	30.80
100	0.15	22.8	9.12	78.52	21.48
200	0.075	20.0	8.00	86.52	13.48
pan	0	33.7	13.48	100.00	

Percentage of coarse aggregate is the percentage passing through size NO 4 (4.75mm) which is given at 2.64%; percentage of medium is given as 100- (13.48+ 2.64) =83.88% and percentage fine aggregate is the percentage passing through the sieve NO 200 (0.075mm) which is 13.48%.

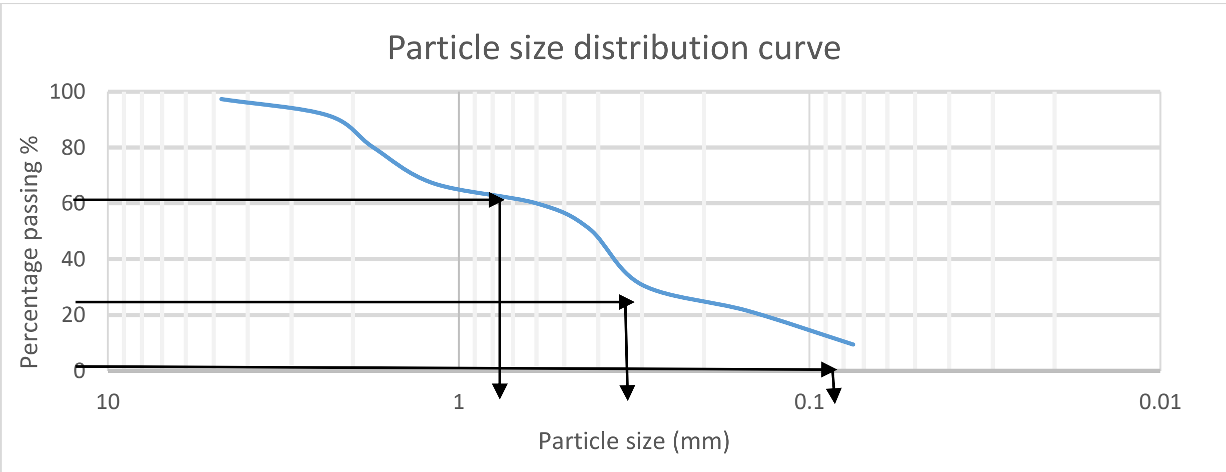

Fig 3.2. Graph for particle size distribution for sample 2

From the above figure 4.2 it can be seen that:
$D_{10} = 0.075$; $D_{30} = 0.287$; $D_{60} = 0.79$; $C_U = 10.48$ and $C_C = 1.39$
The sieve analysis conducted shows the percentage passing for the two soil samples collected the percentage passing through N0 200 sieve for the two samples had a percentage difference of 0.84% with sample 1 having a slightly higher percentage passing than sample 2, the Cc and Cu calculated using the values obtained from the distribution curve above, both samples showed a well graded soil.

3.3 Limit state for sample 1

Table 3.3a: Plastic limit data for sample 1

VARIABLE	Units	1	2
Can number		AI	AI6
Mass of empty can(Mc)	(g)	8.0	8.4
Mass of can & soil (wet) (Mcuc)	(g)	14.7	20.2
Mass of can &soil (dry) (Mcuu)	(g)	13.5	18.3
Mass of soil (Mg)	(g)	5.5	9.9
Mass of water(Mw)	(g)	1.2	1.9
Water content(W)	(%)	**21.81**	**19.19**
AVERAGE		**20.5**	

Table 3.3b. Liquid limit for sample 1

VARIABLE	Units	1	2	3	4
Can number		B28	B21	B38	B14
Mass of empty can(Mc)	(g)	15.0	16.2	11.5	14.3
Mass of can & soil (wet) (Mcuc)	(g)	37.6	37.4	38.3	28.5
Mass of can &soil (dry) (Mcuu)	(g)	33.1	32.2	31.2	24.3
Mass of soil (Mg)	(g)	18.1	16.0	19.7	10.0
Mass of water(Mw)	(g)	4.5	5.2	7.1	4.2
Water content(W)	(%)	**24.86**	**32.5**	**36.04**	**42.0**
No of Blows		39	30	17	10

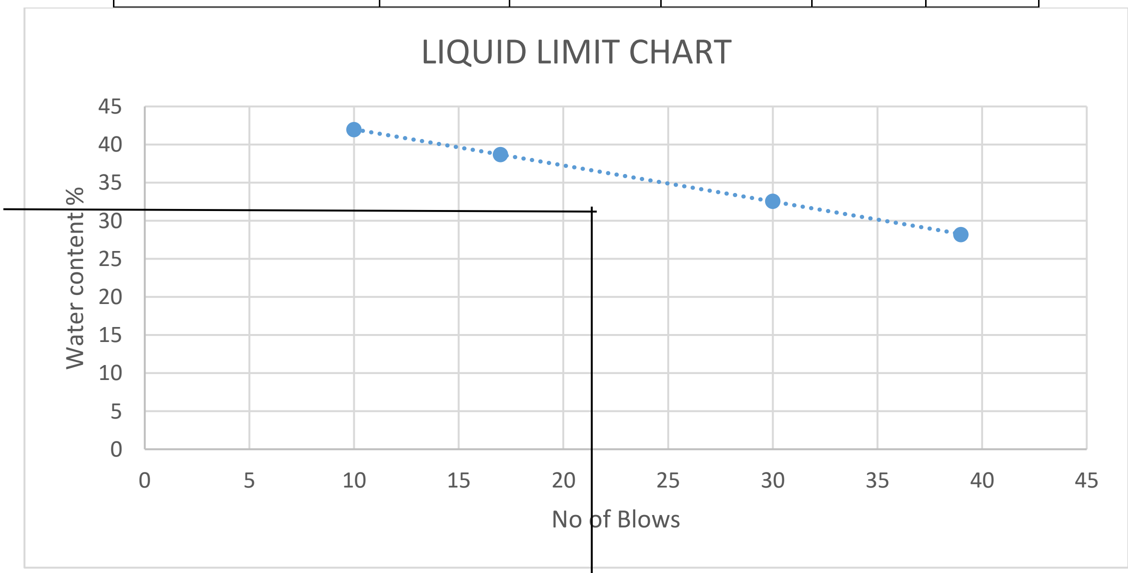

Fig 3.3. Liquid limit chart for sample 1

From the chart above the liquid limit is 35
PI= LL-PL = 35-20.5 = 14.5

3.4 Result for Limit states for Sample 2

Table 3.4a. Plastic limit data for sample 2

VARIABLE	Units	1	2
Can number		A23	A3
Mass of empty can(Mc)	(g)	8.2	8.0
Mass of can & soil (wet) (Mcuc)	(g)	16.2	20.8
Mass of can &soil (dry) (Mcuu)	(g)	14.4	18.7
Mass of soil (Mg)	(g)	6.2	10.7
Mass of water(Mw)	(g)	1.8	2.1
Water content(W)	(%)	**29.0**	**19.6**
AVERAGE		**24.3**	

Table 3.4b. Liquid limit data for sample 2

VARIABLE	Units	1	2	3	4
Can number		B24	B1	B41	B13
Mass of empty can(Mc)	(g)	15.2	12.8	11.4	10.5
Mass of can & soil (wet) (Mcuc)	(g)	39.1	28.1	25.7	28.5
Mass of can &soil (dry) (Mcuu)	(g)	35.0	24.9	21.8	23.2
Mass of soil (Mg)	(g)	19.8	15.3	10.4	12.7
Mass of water(Mw)	(g)	4.1	3.2	3.9	5.3
Water content(W)	(%)	**16.0**	**26.44**	**37.50**	**41.7**
No of blows		39	30	17	10

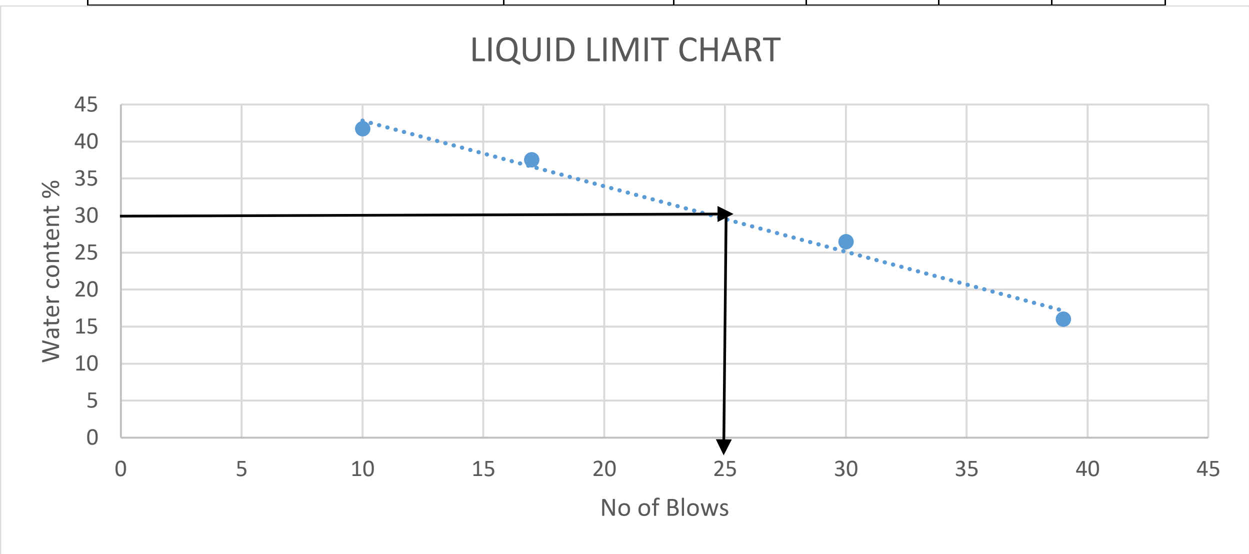

Fig 3.4. Liquid limit chart for sample 2

From the above chart it is determined that:
LL = 30%; PL = 24.3
PI= LL-PL = 30 - 24.3 = 5.7

Table 3.5. Limit State Analysis

Sample 1	Sample 2
Liquid limit(LL)= 35.0%	Liquid limit(LL)= 30.0%
Plastic limit(PL)= 20.5%	Plastic limit(PL)=24.3%
Plasticity index(PI)= 14.5%	Plasticity index(PI)= 5.7%

The Table 3.5 showed the presentation of results for the Atterberg limits for the two soil sample giving the Liquid limit, plastic limit and plasticity index for the soil samples, results from above shows a percentage difference of 15.38% for the Liquid limits of the two samples, 16.96% difference for the plastic limit and a significant percentage difference of 87.12% for the plasticity index.

Table 3.6. Index properties of soils

S/N			SAMPLE 1	SAMPLE 2
1	Atterberg/ consistency limits	LL (%) PL (%) PI (%)	35 20.5 14.5	30.0 24.3 5.7
2	Sieze Analysis	% passing sieze NO 200 (0.075mm)	14.2	13.5
3	AASHTO classification		A-2-4	A-2-6
4	USCS classification		SM	SC

Table 3.6 gives the index properties for the two soil samples for the purpose of classification based on AASHTO and USCS

3.7 Specific Gravity

Table 3.7a. Specific gravity Data sample 1

S/No			BOTTLE	
			A	B
1.	Wt. of Empty bottle	M_1 (g)	34.70	36.10
2.	Wt. of Bottle + Soil	M_2 (g)	44.70	45.80
3.	Wt. of Bottle + soil + Water	M_3 (g)	98.66	106.72
4.	Wt. of Bottle + Water	M_4 (g)	92.48	100.68

BOTTLE 1A

$$\text{Specific gravity (GS)} = \frac{\mathbf{M_2 - M_1}}{\mathbf{(M_4 - M_1) - (M_3 - M_2)}}$$

Specific gravity (GS) = **2.62**

BOTTLE 1B

$$\text{Specific gravity (GS)} = \frac{\mathbf{M_2 - M_1}}{\mathbf{(M_4 - M_1) - (M_3 - M_1)}}$$

Specific gravity (GS) = **2.65**

$$\text{Average GS} = \frac{2.62+2.65}{2} = \mathbf{2.63}$$

Table 3.7b. Specific gravity data for sample 2

S/No			BOTTLE 2	
			A	B
1.	Wt. of Empty bottle	M_1 (g)	34.85	36.60
2.	Wt. of Bottle + Soil	M_2 (g)	43.88	48.70
3.	Wt. of Bottle + soil + Water	M_3 (g)	98.36	112.32
4.	Wt. of Bottle + Water	M_4 (g)	93.02	104.47

BOTTLE 2A

$$\text{Specific gravity (GS)} = \frac{\mathbf{M_2 - M_1}}{\mathbf{(M_4 - M_1) - (M_3 - M_2)}}$$

Specific gravity (GS) = 2.45

BOTTLE 2B

$$\text{Specific gravity (GS)} = \frac{\mathbf{M_2 - M_1}}{\mathbf{(M_4 - M_1) - (M_3 - M_2)}}$$

Specific gravity (GS) = 2.85

$$\text{Average GS}=\frac{2.45+2.85}{2}=\mathbf{2.65}$$

3.8 Preliminary Test Results Summary

Table: 3.8. Summary of Results

S/No.	Experiment		Sample 1	Sample 2
1.	Consistency/ Atterberg Limit Test	LL% PL% PI%	35.0 20.5 14.5	30.0 24.3 5.7
2	Sieve Analysis	Coarse aggregate medium Fine aggregate	2.48% 83.2% 14.32%	2.64% 83.88% 13.48%
		Total	100%	100%
3	Specific Gravity	Gs	2.63	2.65

The Table 3.8 indicates the various results obtained for the experiments carried out from the consistency limits which indicates a liquid limit of 35% and plasticity index of 14.5% for sample 1 and 30% for liquid limit, plasticity index of 5.7% for sample 2, results from above shows a percentage difference of 15.38% for the Liquid limits of the two samples, 16.96% difference for the plastic limit and a significant percentage difference of 87.12% for the plasticity index. The results indicate a higher value in both cases for in sample 1 but the specific gravity for sample 1 has a slightly lower value than sample 2 with a percentage difference of 0.76%.

3.9. Finite Element Analysis Results

The analysis was carried out using SEEP/W for a numerical model of an earthen dam with a base of 35m and elevation of 9m with its top width as 4m also considering a toe drain on the downstream side, the seepage flow determined for earthen dams made up the two soil samples using data obtained from the laboratory results. The seepage flow was obtained from the homogenous earthen dam, the dam made of core with hydraulic conductivity 10 times less than that of the earthen material and also for core with hydraulic conductivity 100 times less taken k for the homogenous material as constant with a value of 1.0 x 10^{-5} m/sec as that of the homogenous earthen material. Results were obtained for both soil samples.

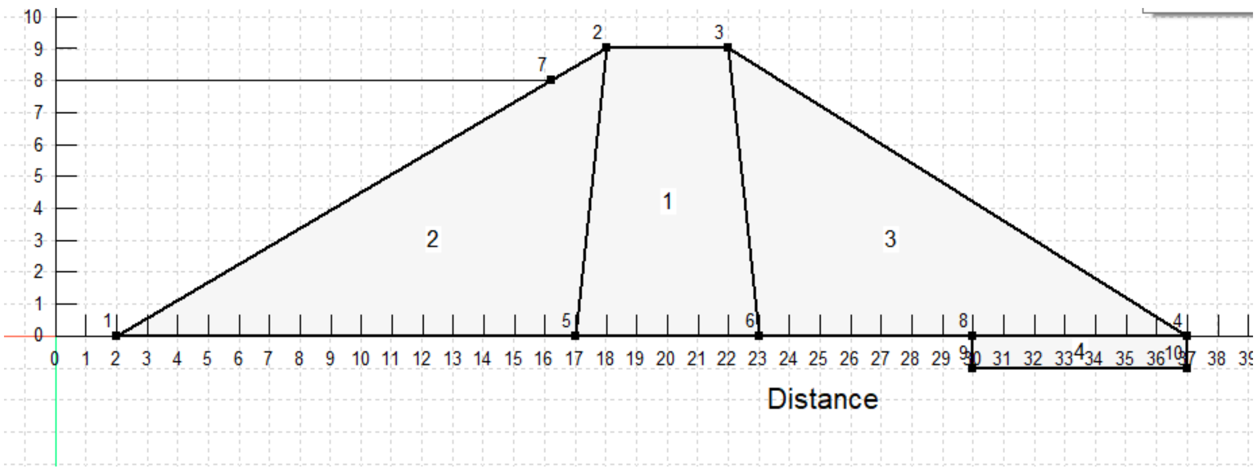

Fig 3.9a. Numerical model of an earthen dam using SEEP/W

The Figure 3.9a represents the model for the numerical analysis before the materials and the boundary conditions for the homogenous dam has been defined, and also does not include the core for the embankment. The above displays the geometry showing the dimensions for all regions of the dam including the water head, base, toe drain and dimensions for the core.

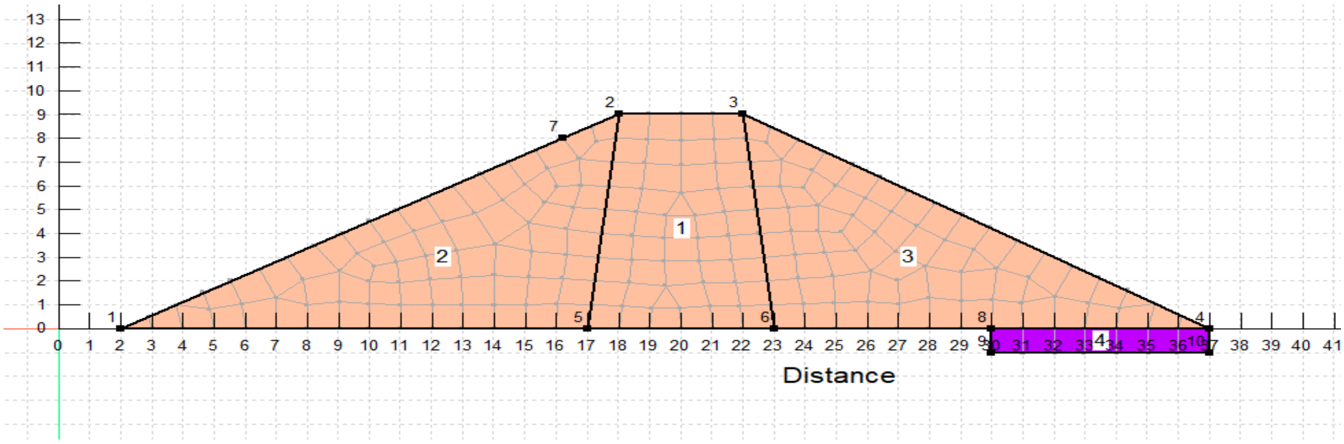

Fig 3.9b. Numerical model of an earthen dam using for sample one without core

This Figure 3.9b showed the indication of the material and boundary conditions for the embankment and toe drain showing the mesh in the model, the difference of color of the embankment and toe drain signifies the different materials used for each of them respectively.

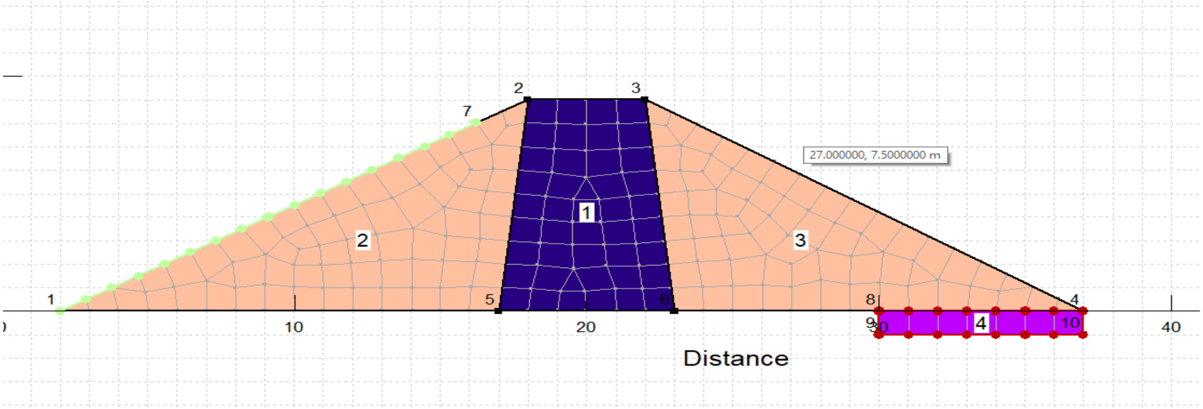

Fig 3.9c. Numerical model for earthen dam sample with core k 10x less

The Figure 3.9c represents the model for embankment with mesh shown and boundary conditions with the inclusion of the core with hydraulic conductivity k 10 times less than that of the homogenous material, the different color code indicates the difference in material for each region the homogenous region, the core and the toe drain.

.

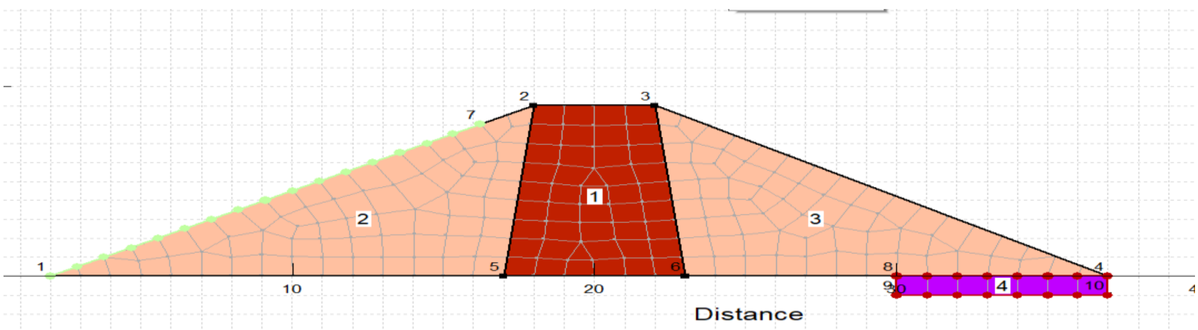

Fig3.9d.Numerical model for earthen dam sample with core k 100x less

The Figure 3.9d represents the model for embankment with mesh shown using an approximate global element size of 1m and boundary conditions with inclusion of the core with hydraulic conductivity k 100 times less than that of the homogenous material, as seen from the fig 3.9b and 3.9c it can be noticed that the core of both is of different color as they are of different materials and hydraulic conductivity respectively, the different color code indicates the difference in material for each region the homogenous region, the core and the toe drain.

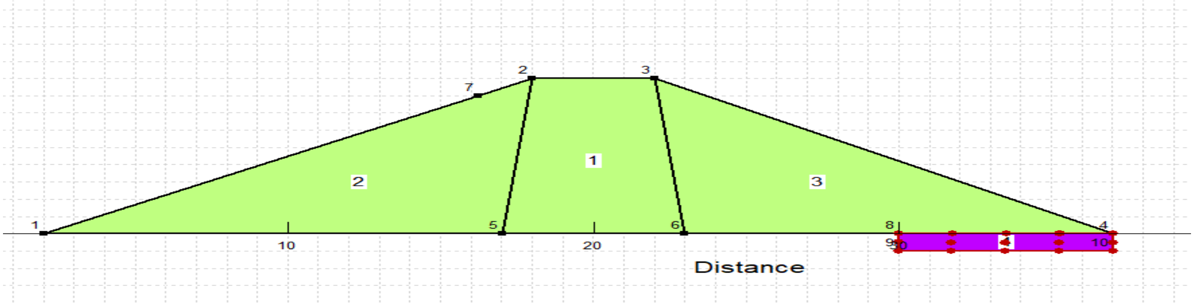

Fig 3.9e. Numerical model of an earthen dam using for sample two without core

This 3.9e shows the indication of the material and boundary conditions for the embankment and toe drain without showing the mesh in the model indicating the various regions of the model by means of number 1,2,3,4 as seen from the figure 3.9d by 1. 2 and 3 representing the homogenous material and 4 representing the toe drain for the dam.

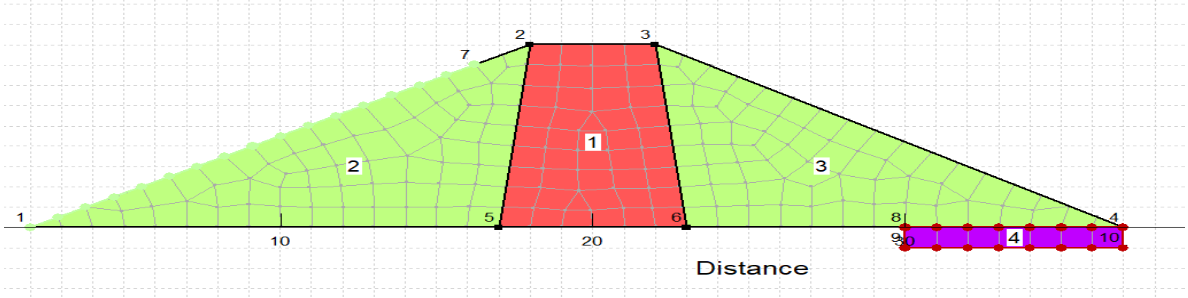

Fig 3.9f. Numerical model of earthen dam for sample two with core k 10x less

The Figure 3.9f represents the model for embankment with mesh shown and boundary conditions with the inclusion of the core with hydraulic conductivity k 10 times less than that of the homogenous material, the different color code indicates the difference in material for each region the homogenous region, the core and the toe drain.

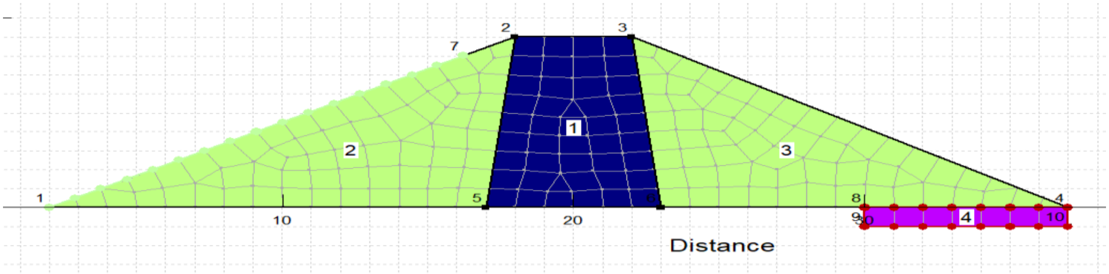

Fig 3.9g. Numerical model of earthen dam sample two k 100x less

The Figure 3.9g represents the model for embankment with mesh shown using an approximate global element size of 1m and boundary conditions with inclusion of the core with hydraulic conductivity k 100 times less than that of the homogenous material, as seen from the fig 3.9e and 3.9f it can Be noticed that the core of both is of different color as they are of different materials and hydraulic conductivity respectively, the different color code indicates the difference in material for each region the homogenous region, the core and the toe drain.

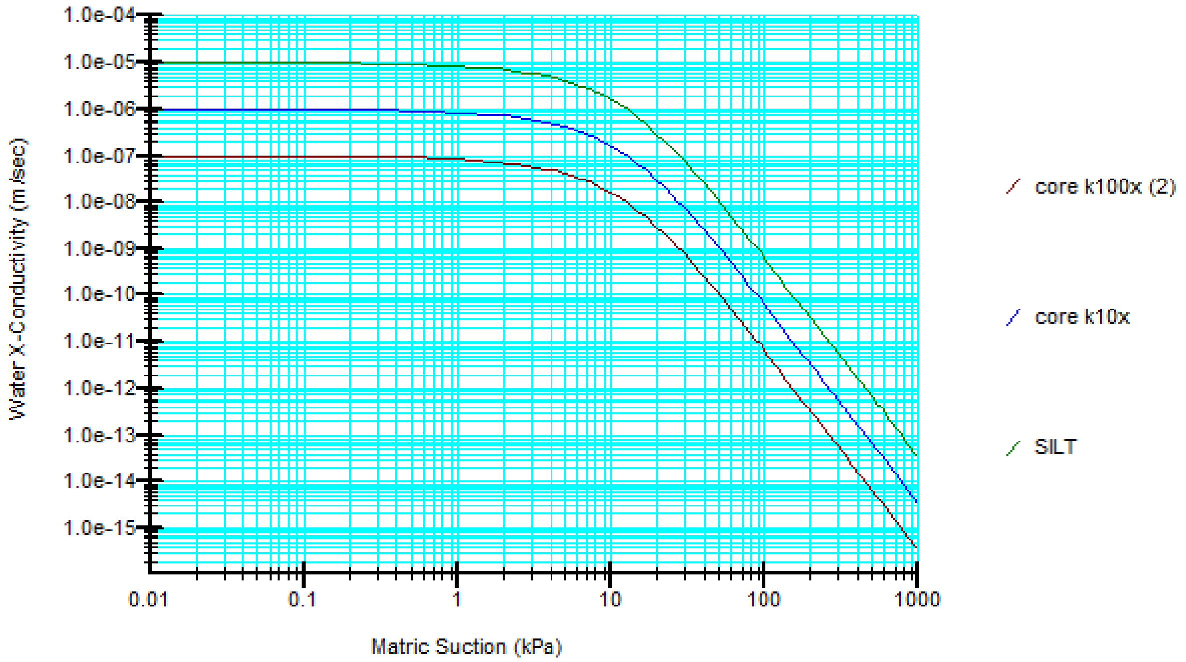

Fig 3.9h. Hydraulic conductivity graph for sample 1

The Figure 3.9h depicts the graph of hydraulic conductivity for the various material region of the model for the homogenous material, the core of the dam with hydraulic conductivity of k 10 times less than that of the homogenous material and the core with hydraulic conductivity of core 100 times less than that of the hydraulic conductivity, the graph was plotted with the matric suction function and indicates a steady rate in the hydraulic conductivity for matric suction between 0.01 and about 5 kPa but after that point the hydraulic conductivity for all materials started to decline increasingly.

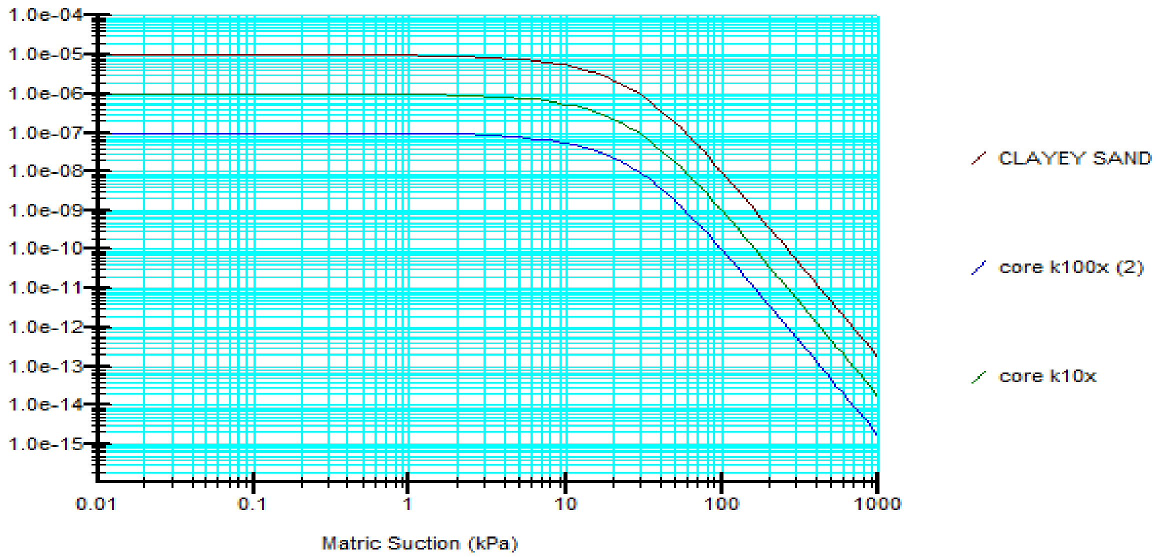

Fig 3.9i. Hydraulic conductivity graph for sample 2

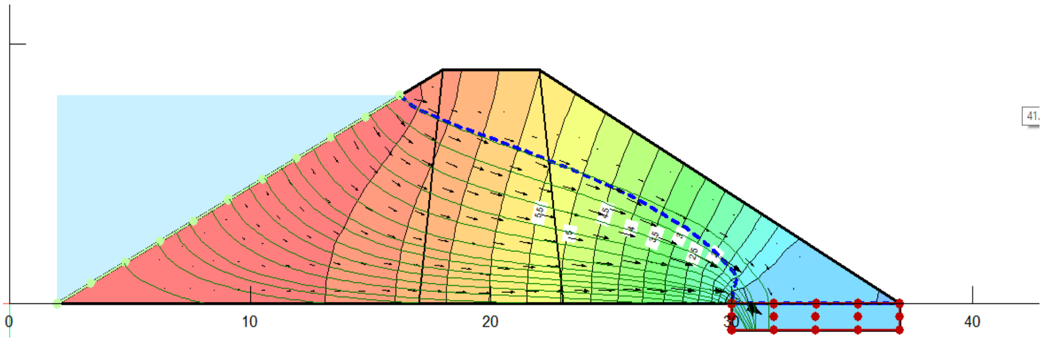

Fig 3.9j. Seepage flow for homogenous earthen dam without effect of core

The Figure 3.9j indicates the result of seepage analysis for the model with only the homogenous materials considered and no core with the effect of the toe drain which is saturated it can be seen from the above the figure the phreatic line which is the top line of seepage and the various flow lines the possible seepage path all going towards the toe drain which serves as a means of collection for the seepage flow, the different colors there indicates the contour for the total water head with red being the region with higher concentration and blue indicating the lower concentration.

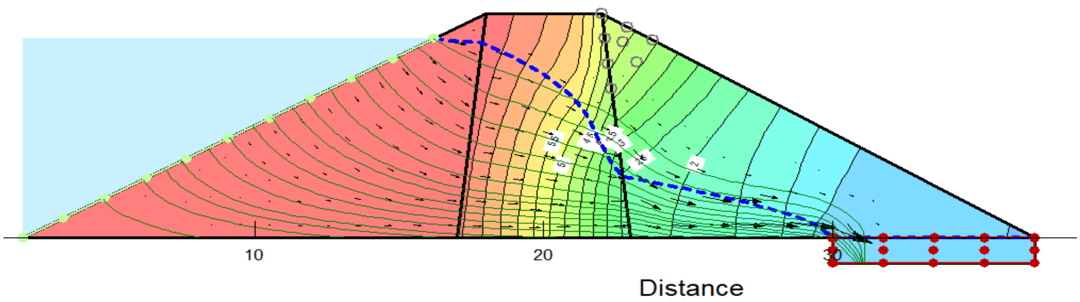

Fig 3.9k. Seepage flow through earthen dam with core of K 10x less

The figure 3.9k indicates the result of seepage analysis for the model with the homogenous materials considered and also the effect of the core with hydraulic conductivity 10 times less than that of the homogenous material, with the effect of the toe drain which is saturated it can be seen from the above the figure the phreatic line which is the top line of seepage and the various flow lines the possible seepage path all going towards the toe drain which serves as a means of collection for the seepage flow, the flow lines differ from that of the fig 3.9j and the total water head is reduced as the flow passes through the core, the different colors there indicates the contour for the total water head with red being the region with higher concentration and blue indicating the lower concentration.

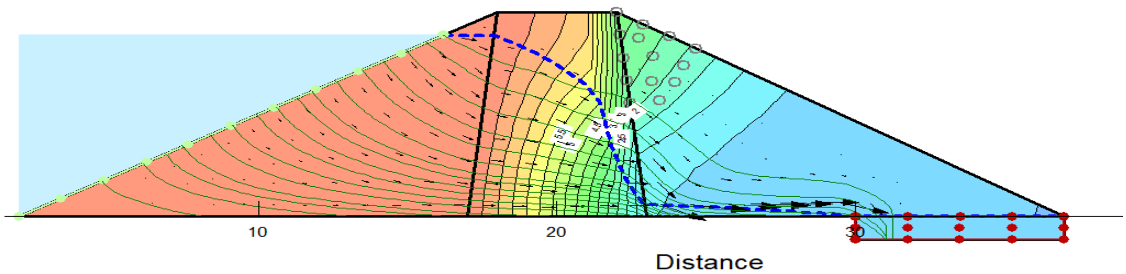

Fig 3.9l. Seepage flow through earthen dam with core of K 100x less

The figure 3.9l indicates the result of seepage analysis for the model with the homogenous materials considered and also the effect of the core with hydraulic conductivity 100 times less than that of the homogenous material, with the effect of the toe drain which is saturated it can be seen from the above the figure the phreatic line which is the top line of seepage and the various flow lines the possible seepage path all going towards the toe drain which serves as a means of collection for the seepage flow, the flow lines differ from that of both the fig 3.9j and 3.9k as the total water head is reduced more as the flow passes through the core, the different colors there indicates the contour for the total water head with red being the region with higher concentration and blue indicating the lower concentration.

Table 3.10. Data for Seepage Flow through the Dam

Seepage	Homogenous dam without core(m^3/sec)	With core of hydraulic conductivity k 10x of earthen material (m^3/sec)	With core of hydraulic conductivity k 100x of earthen material (m^3/sec)
Sample 1	2.41×10^{-6}	2.81×10^{-7}	1.22×10^{-8}
Sample 2	2.72×10^{-6}	2.32×10^{-7}	1.02×10^{-8}
Hydraulic conductivity	1.0×10^{-5}	1.0×10^{-6}	1.0×10^{-7}

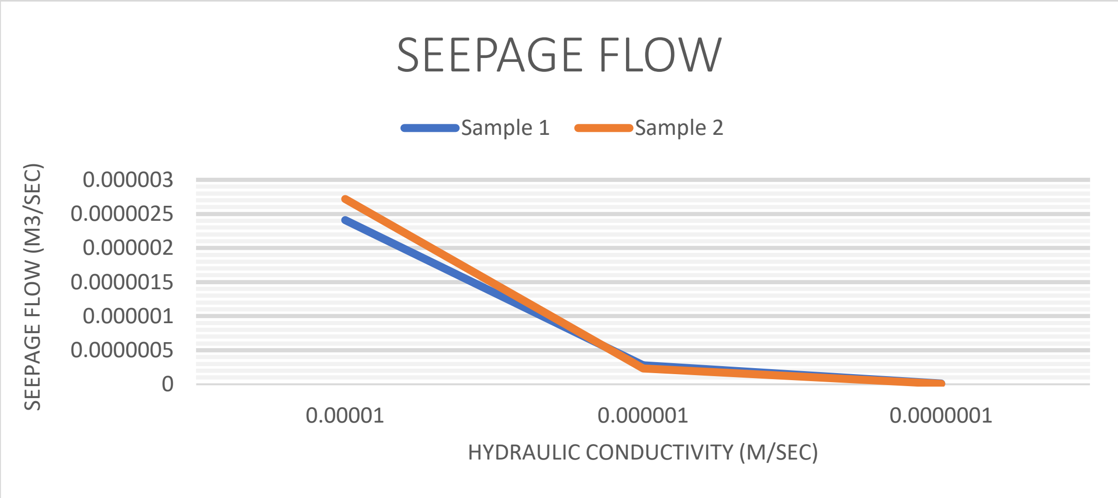

Fig 3.10. Graph of seepage flow for two samples

The above Table 3.10 shows the various seepage flow through the earthen dam of different homogenous material and also considering the effect of core with hydraulic conductivity k at a value 10 and 100 times, respectively that of the homogenous material and the graph showing the seepage flow through the two soil samples indicating the relationship in the rate of flow of seepage with each decrease in hydraulic conductivity. It can be seen that as the hydraulic conductivity of the core decreases the rate of flow of seepage also reduces and at the point of intercept of the two samples from the graph the rate of flow of seepage is the same for hydraulic conductivity at that point. For the hydraulic conductivity of 1 x 10^-5 m/sec for the two samples it can be seen that although the rate of flow of seepage for the two samples is different, they are still respectively higher than that hydraulic conductivity with 10 times less than that of the homogenous material.

The seepage flow through sample one and two has a percentage difference of 12% in the seepage through the earthen material or the homogenous region showing a small but significant difference in rate of flow of seepage, the seepage flow for core with hydraulic gradient of k 10 times less that of the homogenous material has a percentage difference of 19.06% and the rate of flow of seepage for core of hydraulic gradient of k 100 times has a percentage difference of 17.86%.

4.1. CONCLUSION

Laboratory test were conducted to determine some geotechnical properties of the two samples of soil results obtained were used in the numerical modelling for the seepage analysis using the SEEP/W software, the geotechnical properties of the soil were determined and the soil classified accordingly, the two soil samples showed to be silty sand and clayey sand the values obtained from sieve analysis and the consistency used in the numerical analysis of the seepage flow for two different soil samples of taking into consideration the toe drain and effect of core with reduction in hydraulic conductivity, the results obtained showed that when the core is less permeable than the embankment materials the total water head gets dissipated with the flow through the core with decreasing hydraulic gradients.

It could be seen from the results that in the upstream side of the embankment almost no Water head is dissipated because at the upstream side the material is so much more permeable than the core and the zero pressure is seen to be almost horizontal, the first contour drop happens in the core where all the total head gets lost. Verry little of the total water head gets lost by the flow in the downstream shell this shows how the material properties affects the loss of water head.

The results obtained for the seepage flow through earthen dam plotted in the graph shows the reducing seepage flow with significant decrease in the hydraulic conductivity of the core. Also indicated is the percentage difference of the seepage flow through the two soil materials.

4.2 Recommendations

Based on the results obtained from the research work I recommend that:

i. For earthen dam made of homogenous materials sample two offers a more suitable options as the earthen material than sample one, as the seepage flow through the sample two (clayey sand) is less than that of sample one (silty sand).

ii. For earthen dams to reduce the seepage flow an impervious core with significant reduction in the hydraulic conductivity should be used as the core material.

REFERENCES

1) Abdul Jabbar Jamel, A. (2016). Analysis and Estimation of Seepage through Homogenous Earth Dam without Filter. Diyala Journal of Engineering Sciences, 9(2), 38-49.
2) Adamo, N., Al-Ansari, N., Sissakian, V., Laue, J., & Knutsson, S. (2020). Dam Safety Problems Related To Seepage. Journal of Earth Sciences and Geotechnical Engineering, 10(6), 191-239.
3) Amangabara, G. T., & Obenade, M. (2015). Flood Vulnerability Assessment of Niger Delta States Relative to 2012 Flood Disaster in Nigeria. American Journal of Environmental Protection, 3(3), 76-83.
4) Arinze, E. E., & Agunwamba, J. C. (2010). Comparative Analysis of Seepage through Dam Using Different Analytical and Numerical Methods. Journal of Engineering and Applied Sciences, 6(1-2), 78-87.
5) ASTM International. (2006). Standard Practice for Classification of Soils for Engineering Purposes (Unified Soil Classification System). ASTM D 2487-06.
6) Awomeso, J. A., Ufoegbune, G. C., Gbadebo, A. M., Balogun, G. O., & Eruola, A. O. (2009). Towards Effective Planning, Design and Monitoring of Dams In Nigeria. Journal of Agricultural Science and Environment, 9(2), 45-63.
7) ASTM International. (2006). Standard Practice for Classification of Soils for Engineering Purposes (Unified Soil Classification System). ASTM D 2487-06.
8) Bayat, M., Eslamian, S., Shams, G., & Hajiannia, A. (2019). The 3-D Analysis and Estimation of Transient Seepage in Earth Dams through PLAXIS 3-D Software: Neural Network. Environmental Earth Sciences, 78(18), 1-7.
9) British Standard (BS) 1377 (1975) Methods of test for soils for civil engineering purposes. British Standard Institution, London.
10) British Standard (BS) 1377, Part 2. (1990). Method for the determination of Specific Gravity of Aggregates
11) British Standard 812-103.1: 1985. Testing aggregates. Method for determination of particle size distribution - Sieve tests.
12) Chu-Agor, M. L., Fox, G. A., Cancienne, R. M., & Wilson, G. V. (2008). Seepage Caused Tension Failures and Erosion Undercutting of Hillslopes. Journal of Hydrology, 359(3-4), 247-259.
13) Das, B. M., & Das, B. M. (2008). Advanced soil mechanics (Vol. 270). New York: Taylor & Francis.
14) Earle, S. (2015). Physical Geology. 2nd Ed. Victoria, B.C: BC campus. Canada.
15) Emeka, A. E., & Chukwuemeka, A. J. (2019). Modified Schaffernak’s Solution for Seepage through Earth Dam. Mathematical Modelling and Applications, 3(4), 44.
16) Hoffman, J.D, (2001). Numerical Methods for engineers and Scientists. McGraw-Hill, New York: CRC press.
17) Hosni, A. A., Pauzi, N. I. M., & Shariffuddin, A. S. (2015). Geotechnical Properties of Waste Soil from Closed Construction Dumping Area in Serdang, Selangor, Malaysia. Elect. J. Geotech. Eng. (EJGE), 2015(20), 17.
18) Jairry, H. H. A. (2010). 2-D Flow Analysis through Zoned Earth Dam Using Finite Element Approach. Eng. & Tech. Journal, 28(21).
19) Jie, Y., Jie, G., Mao, Z., & Li, G. (2004). Seepage Analysis Based On Boundary-Fitted Coordinate Transformation Method. Computers and Geotechnics, 31(4), 279-283.
20) Kacimov, A. R., Al-Maktoumi, A., & Obnosov, Y. V. (2021). Seepage through Earth Dam with Clay Core and Toe Drain: The Casagrande–Numerov analytical legacy revisited. ISH Journal of Hydraulic Engineering, 27(sup1), 264-272.
21) Kermani, F. E., & Barani, G. A. (2012). Seepage Analysis Through Earth Dam Based On Finite Difference Method. Journal of Basic and Applied Scientific Research, 2(11), 11621-11625.
22) Komolafe, A. A., Adegboyega, S. A. A., & Akinluyi, F. O. (2015). A Review of Flood Risk

Analysis in Nigeria. American Journal of Environmental Sciences, 11(3), 157.

23) Leontiev, A., & Huacasi, W. (2001). Mathematical Programming Approach for Unconfined Seepage Flow Problem. Engineering Analysis with Boundary Elements, 25(1), 49-56.
24) Li, G., Ge, J., & Jie, Y. (2003). Free Surface Seepage Analysis Based On The Element-Free Method. Mechanics Research Communications, 30(1), 9-19.
25) Magami, I. M. Yahaya, S. and Mohammed, K. (2014). Causes and Consequences of Flooding in Nigeria : A Review. Biological and Environmental Sciences Journal for the Tropics, 11(2).
26) Malkawi, A. I. H., & Al-Sheriadeh, M. (2000). Evaluation and Rehabilitation of Dam Seepage Problems. A case study: Kafrein dam. Engineering Geology, 56(3-4), 335-345.
27) Manning, J. C. (2016). Applied principles of hydrology, 3rd ed. Waveland Press.
28) Oke, I. A., & Abubakar, I. (2013). Dams and Water Supply Systems in Nigeria. Dams: Structure, Performance and Safety Management, 279–292.
29) Okosun, V. A., & Amadasu, A. B. (2016). The Influence of Dams on the Growth and Development of Nigerian Economy. International Journal of Management and Applied Science, 2(1).
30) Olonade, K. A., & Agbede, O. A. (2013). A Study of Seepage through Oba Dam Using Finite Element Method. Civil and Environmental Research, 3(3), 53-60.
31) Onyeka, F. C. (2019). Application of Industrial Waste (Saw-Dust Ash) in the Production of Self-Compacting Concrete. International Research Journal of Innovations in Engineering and Technology (IRJIET), Volume 3(1), 1-9.
32) Onyeka, F. C., Osegbowa Douglas (2020). Soil Structural Analysis of Laterite Properties used as a Road Construction Material, Abuja as a Case Study. International Research Journal of Innovations in Engineering and Technology - IRJIET, 4(11), 35-42. DOI of article https://doi.org/10.47001/IRJIET/2020.411005
33) Panthulu, T. V., Krishnaiah, C., & Shirke, J. M. (2001). Detection of Seepage Paths in Earth Dams Using Self-Potential and Electrical Resistivity Methods. Engineering Geology, 59(3-4).
34) Prakash, K., Sridharan, A., Thejas, H. K., & Swaroop, H. M. (2012). A Simplified Approach of Determining the Specific Gravity of Soil Solids. Geotechnical and Geological Engineering, 30(4), 1063-1067.
35) Salem, M. N., Eldeeb, H., & Nofal, S. (2019). Analysis of Seepage through Earth Dams with Internal Core. Int. J. Eng. Res, 8, 768-771.
36) Salmasi, F., & Abraham, J. (2021). Validity of Schaffernak and Casagrande Analytical Solutions for Seepage through a Homogeneous Earth Dam and Comparison with Numerical Solutions Based on the Finite Element Method. Novel Perspectives of Engineering Research Vol. 4, 79-93.
37) Sazzad, M. M., Roy, M., & Rahman, M. S. (2014). Comparison between Numerical and Analytical Solution of Seepage Flow through Earth Dam. Second International Conference on Advances in Civil Engineering (pp. 300-306).
38) Tezaghi K, Peck K & Mersri G (1996). Soil Mechanic in Engineering Practice. Third Ed., John Wiley and Sons, New York, USA.
39) Torabi Haghighi, A., Tuomela, A., & Hekmatzadeh, A. A. (2020). Assessing the Efficiency of Seepage Control Measures in Earthfill Dams. Geotechnical and Geological Engineering, 38(5), 5667-5680. DOI: doi.org/10.1007/s10706-020-01371-w.
40) Uromeihy, A., & Barzegari, G. (2007). Evaluation and treatment of seepage problems at Chapar-Abad Dam, Iran. Engineering Geology, 91(2-4), 219-228.
41) Watanabe, S., Kim, H., & Kanae, S. (2013). Global Ood Risk under Climate Change. Nat Clim Change, 3(9), 816821. DOI: 10.1038/nclimate1911
42) Wang, E. (2013). Damning the Dams: A Study of Cost Benefit Analysis in Large Dams through the Lens of India's Sardar Sarovar Project.
43) Zhou, P. B. (2012). Numerical analysis of electromagnetic fields. Springer Science & Business Media.